

# Seismic response of curve bridge with frictional pendulum system under multidimensional seismic excitation

**Abstract:** This study examines the impact of multidimensional seismic excitation on the seismic performance of a curved bridge utilizing a friction pendulum. A finite element model of a four-span curved simply supported beam girder is developed using Sap2000. The analysis focuses on the influence of the seismic wave's characteristic period and the friction coefficient of the friction pendulum on the seismic response of vibration-isolated bridges, employing the nonlinear time-distance method. The findings indicate that the characteristic period of seismic waves exerts varying effects on distinct locations of the bridge structure, with vertical seismic waves significantly impacting the seismic response of the abutment structure. Furthermore, as the friction coefficient escalates, the varying dimensions of seismic waves increasingly affect different locations of the bridge structure, while the seismic response of the abutment follows a consistent pattern of change.

**Keywords:** curved bridge; characteristic period; friction pendulum system; seismic response

## 1. Introduction

Curved bridges are essential for linking highways and urban roadways, as they

accommodate diverse topographical needs while also exhibiting aesthetic appeal. The seismic response analysis of curved bridges cannot be readily inferred from that of straight bridges due to the former's more intricate geometric arrangement. Khashayar et al. determined that the abutment characteristics and boundary conditions of curved bridges significantly influence the assessment of their seismic response in contrast to straight bridges, and the application of equivalent straight bridges becomes increasingly limited with higher seismic intensity levels [1].

The orientation of seismic waves during an earthquake is highly unpredictable. The orientation of seismic waves is typically defined in curved bridges as downward, transverse, and vertical. Research on the impact of seismic waves on linear bridges is well-documented; however, there is a paucity of studies examining the influence of multidimensional seismic waves on curved bridges on standard roadways. Swagata [2] determined that the safety requirements for a bridge are most critical when seismic waves propagate horizontally at an angle of  $30^\circ$  to  $60^\circ$  relative to the bridge's longitudinal axis. Nielson, B. G. [3], Xiao Liang et al. [4] examined the significance of both longitudinal and transverse seismic waves in concrete-dominated highway bridges, which are susceptible to fractures at the junctions of the abutments and main girders, necessitating scrutiny. Li et al. [5] and Cai et al. [6] investigated the seismic behavior of continuous curving bridges under horizontal bi-directional seismic forces. The findings indicate that solely accounting for unidirectional seismic input will lead to an underestimation of the seismic reaction and potential damage to the structure, resulting in an inaccurate evaluation of the bridge's seismic performance. Furthermore,

the dynamic response of bridge structures to two-dimensional horizontal seismic actions is significantly greater than that to one-dimensional actions, attributable to the increased dimensionality of seismic waves.

The examination of three-dimensional seismic waves has amplified the impact of vertical ground shaking on bridges relative to two-dimensional seismic wave activity. Progress has been achieved in evaluating the impact of 3D seismic waves on the seismic response of bridges. Sunil Thapa et al. [7], Chen et al. [8-9] examined the impact of multidimensional factors on the seismic response of bridges. The findings indicate that it is impractical to disregard the influence of vertical seismic forces on bridges. Furthermore, several failure modes are delineated, encompassing damage to the bridge superstructure, vertical separation and impact, bending damage, decreased friction, and shear bond failure, among others. Zhang et al. [10] and Zite L et al. [11] examined the seismic response of arch bridges subjected to multidimensional ground shaking and concluded that reinforcement of the central structure of the arch bridge is necessary. Wang et al. [12], Zeynep Gulerce et al. [13], Zhang et al. [14], Yan [15] et al. examined the seismic response of multi-dimensional ground shaking on cable-stayed bridges, conventional highway bridges, and Y-type bridges. Their findings indicate that both horizontal and vertical seismic actions must be concurrently addressed in seismic design, with vertical ground shaking notably influencing the axial force of the bridge abutment and the bending moment at the abutment's apex. Thomas Wilson et al. [16] conducted numerical simulations of curved three-span bridges, revealing that vertical ground shaking significantly impacts

these structures in moderately seismic zones. Gu et al. [17] examined the seismic response of large-span isolated structures to multidimensional seismic wave inputs. The horizontal dynamic response was shown to be larger under three-dimensional ground shaking inputs compared to two-dimensional seismic motion input, suggesting that vertical ground shaking enhances the horizontal dynamic response of the structure. Wan et al. [18] investigated the impact of vertical ground shaking on the seismic fragility of bridge-foundation systems, highlighting the specific demand and capacity modeling factors necessary for fragility analysis in this context.

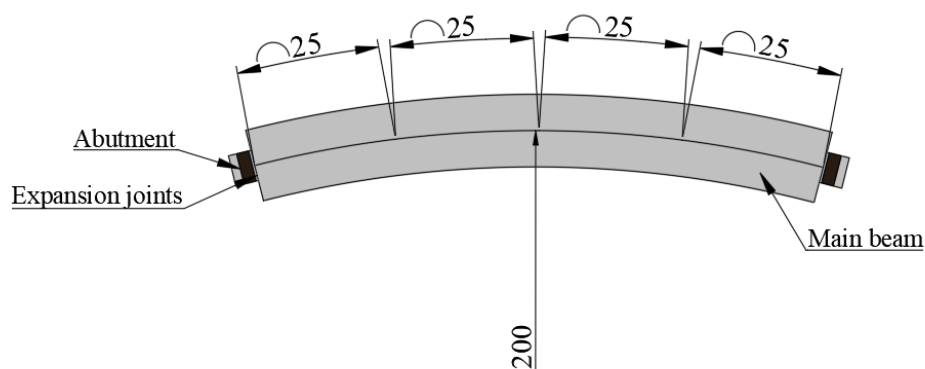
The analysis of results in studies on curved bridges is more diverse due to their greater complexity than that of straight bridges. Ni et al. [19] investigated the seismic response of curved girder bridges in relation to the angle of ground motion input. Different ground vibration input angles were employed to determine the maximal value of the seismic response of curved bridges, and F. Ferreira s [20] investigated the seismic performance of curved cable-stayed bridge. The multicomponent seismic response analysis methods of curved bridges were systematically analyzed and compared by Gao et al. [21], who also investigated the limitations and superiority of the various analysis methods. The impact of spatial variation in ground motion on the nonlinear dynamic response of highway bridges was examined by Vinita SAXENA et al. [22]. Mahmood Minavanda et al. [23] conducted a study on the seismic response of horizontally curved bridges in the presence of near-site vibration. The findings indicated that the abutment's susceptibility in the radial direction of the arc is proportional to the curvature of the bridge deck, which in turn increases the shear

force, bending moment, and displacement of the abutment.

Conversely, this paper examines the impact of the dimensionality of the seismic wave on the structural parameters of the bridge, based on the aforementioned study, and analyzes the variation of the bridge seismic response with the characteristic period of the seismic wave and friction coefficient of the friction pendulum under the action of seismic waves of varying dimensions using the curvilinear bridge model established in sap2000.

## 2. Engineering Overview

The research object of this paper is a standard highway curve bridge. Figure 1 illustrates the schematic diagram of the entire bridge. The radius of the bridge centerline is 200 meters, and the bridge span is 25 meters. The abutment is a circular double-column pier with a diameter of 1.5 m and a pier height of 8 m, while the primary girder is a concrete box girder structure. The expansion joints connect the main girder and the abutments at the two extremities, while the FPS connects the abutments. The structural drawings of the bridge's main girder and piers are depicted in Fig. 1(a) through Fig. 1(d).



(a)

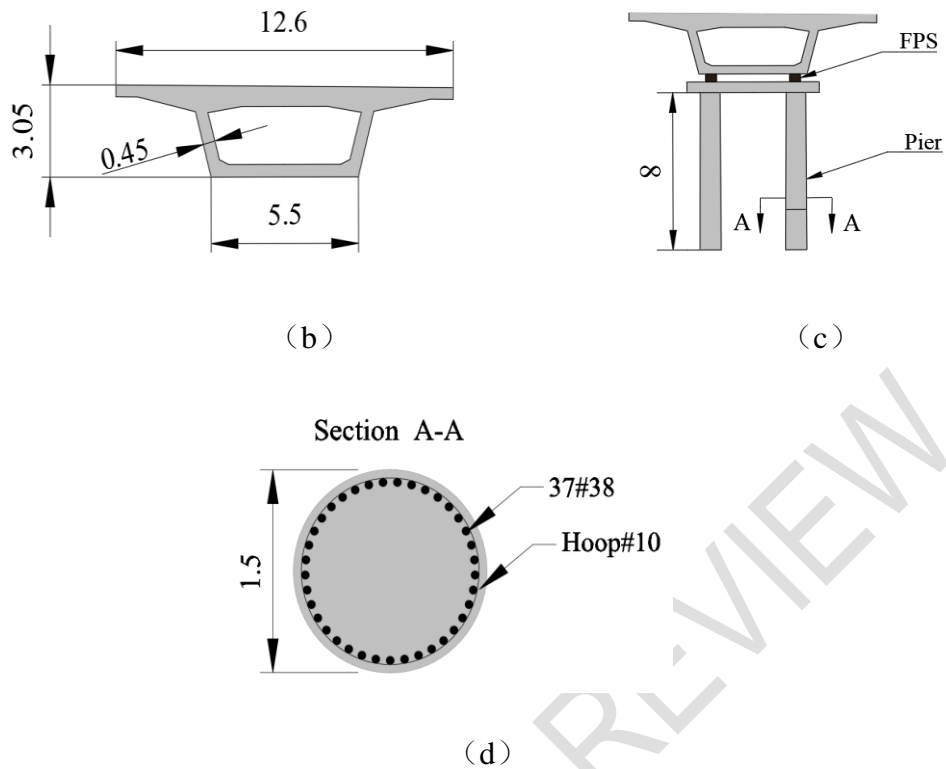


Fig. 1: (a) Top view of the bridge; (b) Sectional view of the abutment; (c) Cross-sectional parameters of the main girder; (d) Sectional view of the abutment.

### 3. Computational Models

#### 3.1 Finite element model

This paper establishes a finite element model of nonlinear dynamics for a 4-span curved simply supported girder bridge with friction pendulum bearings using Sap2000 [24], as illustrated in Fig. 2. The model is converged and verified to ensure that the appropriate mesh density is achieved. These include the following: beam cells are used to simulate the main girders and piers, thick plate cells are used to simulate the abutments, friction pendulum bearings are simulated using friction pendulum cells in Sap2000, Gap cells are used to simulate the expansion joints, and fixed constraints are applied to the bottom of the pile foundations.

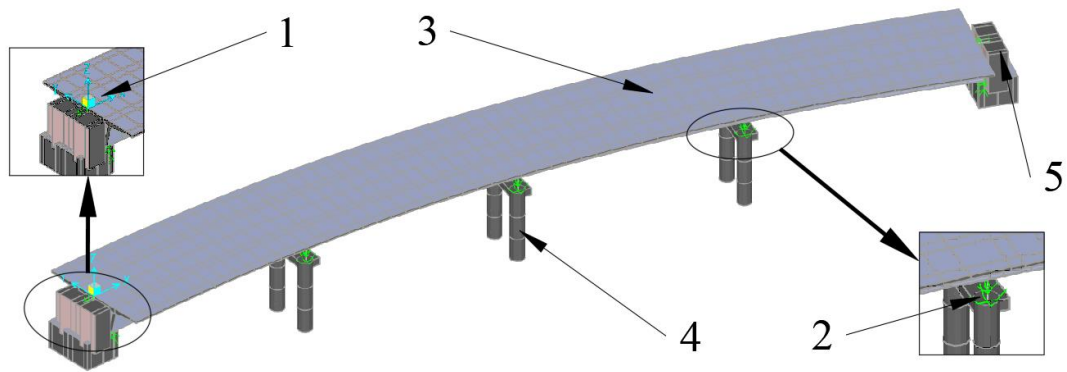


Fig. 2 .3D view of curved bridge (1) abutment; (2) FPS; (3) main girder; (4) abutment; (5) expansion joint.

### 3.2 Seismic Excitation

According to China's seismic design[25] code for bridges, the Class I site category is selected with a seismic intensity of 7 degrees. Three artificial seismic excitations are synthesized using Matlab, featuring a peak acceleration of 0.2g and a characteristic period of 0.25s. Additionally, seismic waves are generated for characteristic periods of 0.25s, 0.35s, 0.45s, and 0.65s, all with the same peak acceleration. Three seismic waves are produced for each characteristic period, and the corresponding acceleration time curves are illustrated in Figures 3. to 6.

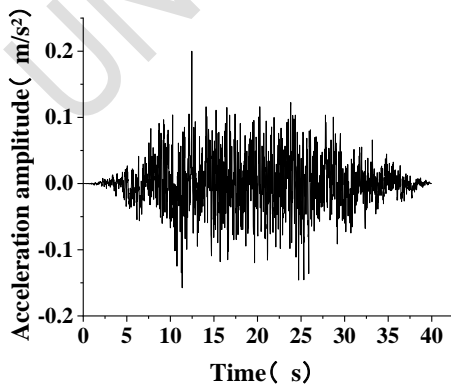


Fig. 3 Period: 0.25s

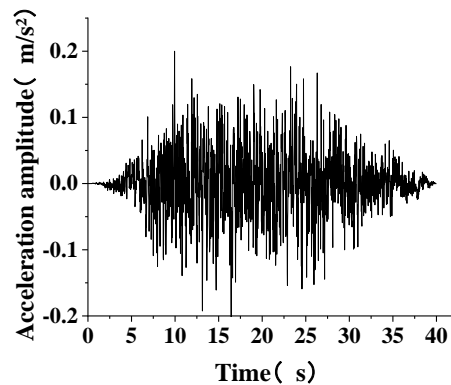


Fig. 4 Period: 0.35s

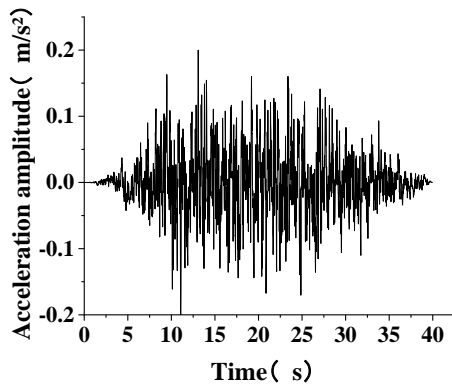


Fig.5 Period: 0.45s

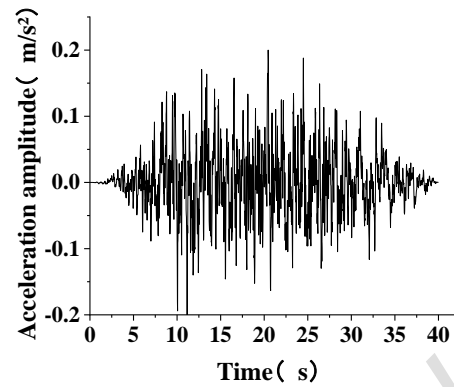


Fig. 6 Period: 0.65s

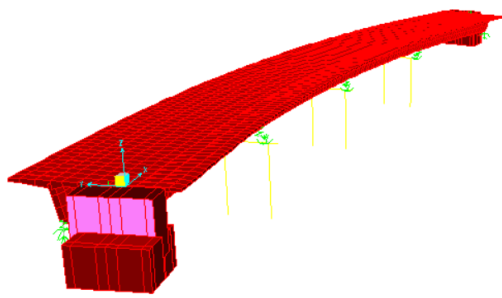
## 4 .Analysis of results

### 4.1 Modal analysis

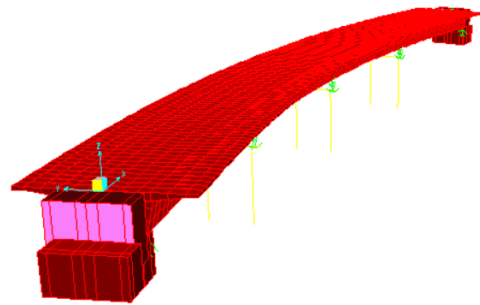
The theoretical formula for the seismic isolation period of the friction pendulum support is shown in equation (1), where  $R$  is the spherical radius of the friction pendulum support and  $g$  is the gravitational acceleration. From equation (1), the theoretical isolation period of the friction pendulum bearing with a spherical radius of 2 m is 2.81 s. The first 6-order vibration pattern of the friction pendulum bearing with a spherical radius of 2 m obtained by numerical simulation is shown in Fig. 3, and it can be seen in Fig. 3 that the isolation period of the bridge obtained by numerical simulation is 2.97 s, which is only 5.7% of the theoretical calculation results.

$$T_p = 2\pi \sqrt{\frac{R}{g}}$$

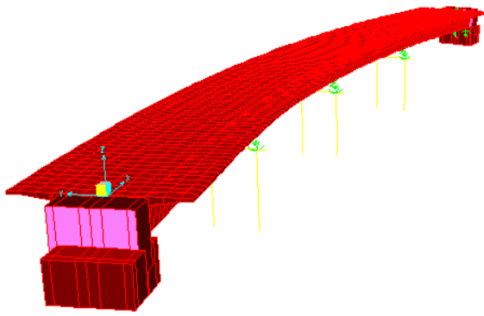




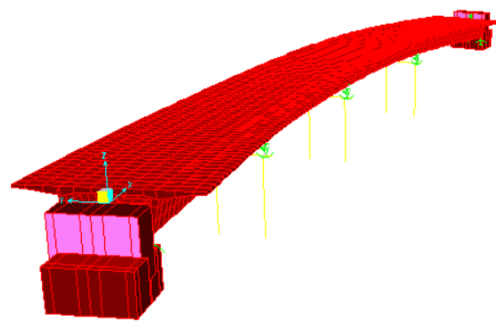
(a) Principal vibration mode of the first order (2.97s)



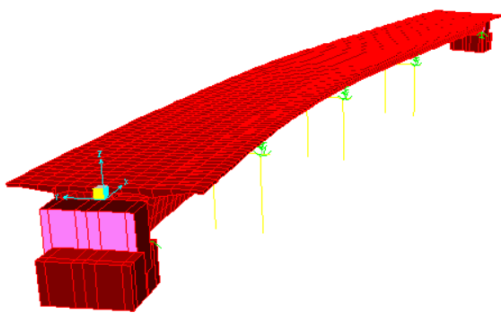
(b) Principal vibration mode of the second order (2.18s)



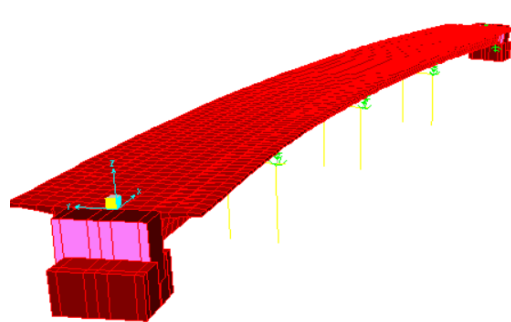
Principal vibration mode of the first order (2.97s)



(d) Principal vibration mode of the first order (2.97s)



(e) Principal vibration mode of the first order (2.97s) (0.47s)



(f) Principal vibration mode of the first order (2.97s) (0.29s)

Fig 7: The initial six modes of vibration

#### 4.2.Simulation analysis of a friction pendulum simply supported girder bridge

## subjected to multi-dimensional seismic excitation

Each datum is derived by averaging three seismic waves with identical characteristic periods. The subsequent picture illustrates the displacement variation of the primary beam in relation to the characteristic period under the influence of a one-dimensional seismic wave.

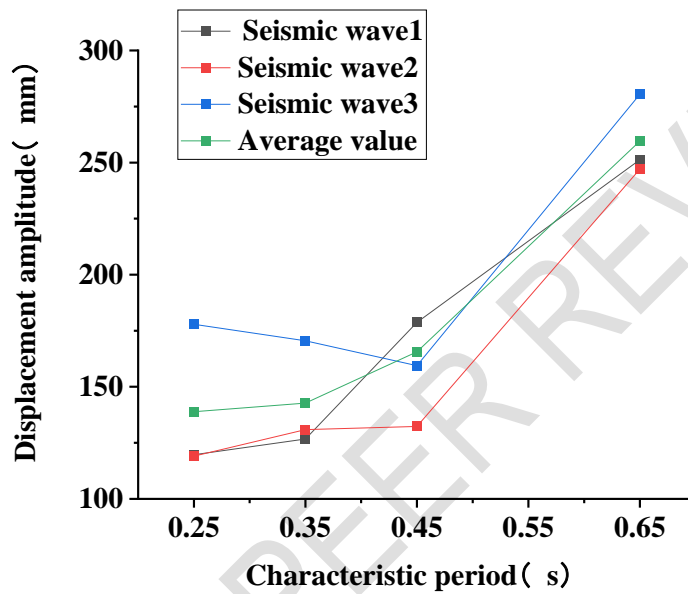


Fig. 8 Example of result processing

### 4.2.1 Examination of the impact of characteristic period on bridge seismic response under multidimensional seismic stimulation

This section examines the impact of the characteristic period of seismic waves on the seismic response of simply supported beams subjected to seismic waves of varying dimensions. A friction coefficient of 0.05 for the friction pendulum is employed, and artificial seismic excitation is utilized for simulation and analysis. The results of the calculations are presented below.

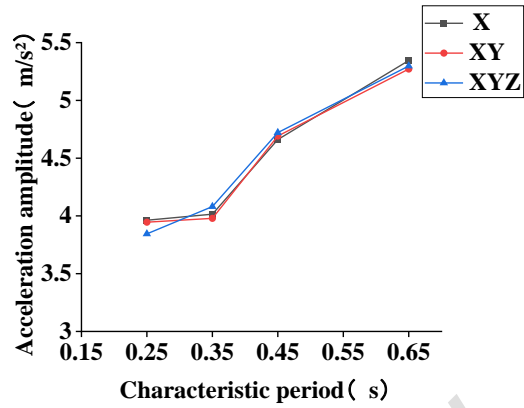
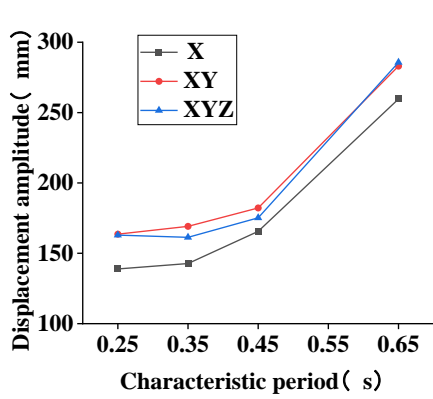


Fig. 9: Displacement of the Main Beam      Fig. 10: Acceleration of the Main Beam

Figure 9 illustrates that, when subjected to various dimensional seismic waves, the displacement of the main beam escalates with the elongation of the characteristic period of the seismic waves. Notably, the displacement values of the main beam under the influence of seismic waves in the XY and XYZ directions exceed those observed in the X direction. Figure 10 illustrates that as the characteristic period of the seismic wave increases, the acceleration value of the main beam rises under the influence of seismic waves of varying dimensions. Furthermore, the acceleration values of the main beam under different seismic wave dimensions are approximately equivalent at the same characteristic period, with a maximum discrepancy of 3%.

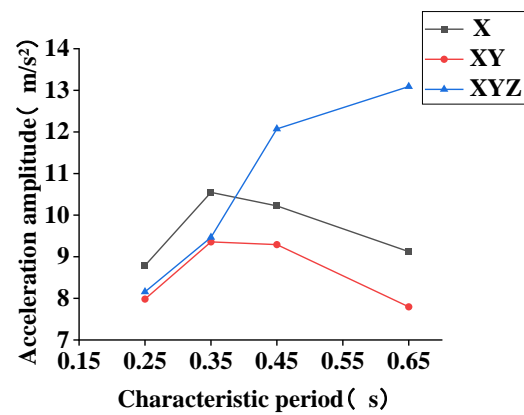
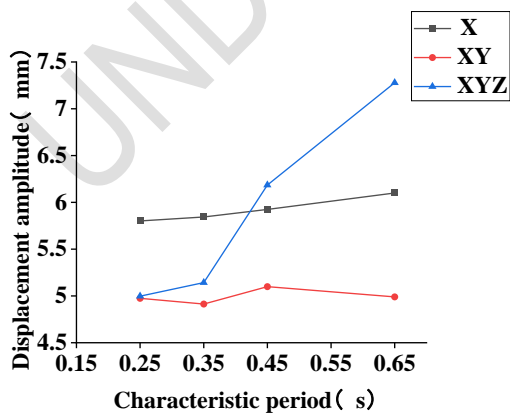


Fig. 11: Displacement of the pier top      Fig. 12: Acceleration of the pier top

Figure 11 illustrates that as the characteristic period of the seismic wave

increases, the maximum rate of change in the X-direction pier top displacement reaches 5.1%, the maximum rate of change in the XY-direction pier top displacement attains 3.8%, while the XYZ-direction pier top displacement exhibits an upward trend, with a maximum rate of change of 45.6%. The vertical seismic wave significantly influences the displacement of the pier top. Figure 12 illustrates that as the characteristic period of the seismic wave increases, the acceleration value at the top of the pier in the X direction exceeds that of the XY direction, with the latter initially rising and then declining. This trend is consistent across both measurements. At a characteristic period of 0.35 seconds, both reach their maximum values, with a maximum rate of change of 20%. The acceleration value at the top of the pier in the XYZ direction exhibits an upward trend, surpassing the values in the X and XY directions at a characteristic period of 0.45 seconds, with a maximum change rate of 60.5%.

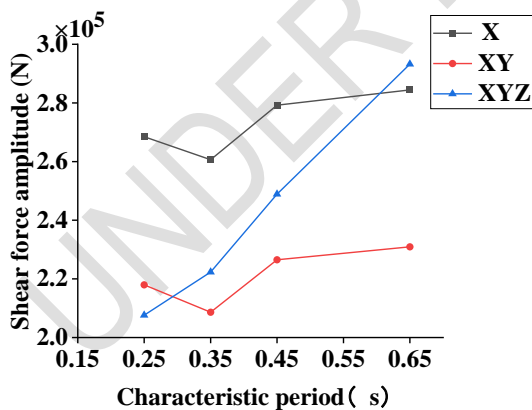


Fig. 13: Shear force at the pier bottom

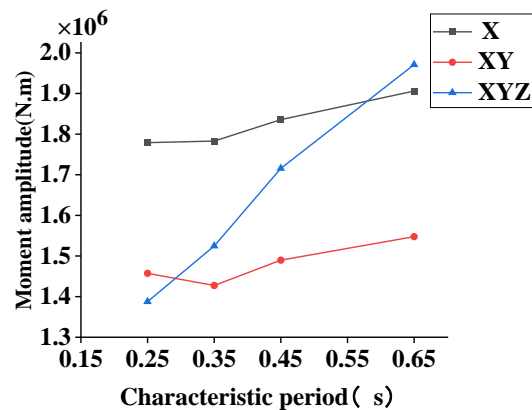


Fig. 14: Bending moment at the pier bottom

Figures 13 and 14 illustrate that as the characteristic period of the seismic wave increases, the shear force and bending moment values at the pier bottom in the X

direction and XY direction initially decrease and then increase, with the values in the X direction exceeding those in the XY direction; the trend in the XYZ direction consistently rises. The maximum rates of change for the shear force values at the pier bottom are 9.1% in the X direction, 10.7% in the XY direction, and 41.2% in the XYZ direction. The maximum rates of change for the bending moment values at the pier bottom are 7.1% in the X direction, 8.4% in the XY direction, and 42% in the XYZ direction. The percentages for the X direction, XY direction, and XYZ direction are 7.1%, 8.4%, and 42%, respectively.

#### 4.2.2 Impact of friction coefficient on bridge structural characteristics subjected to multidimensional seismic wave inputs

In order to study the effect of friction coefficient on the seismic performance of simply supported girder bridges in this section, the characteristic period of 0.25s and friction coefficients of 0.01~0.12 are selected for seismic response analysis.

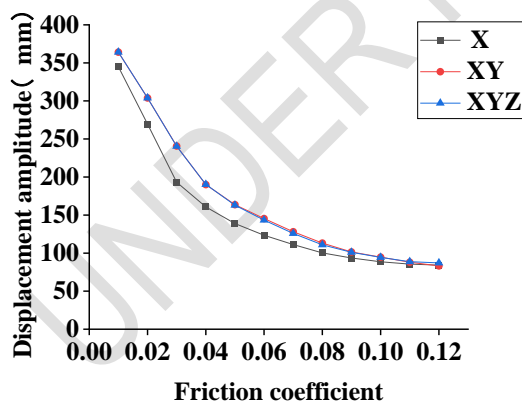


Fig. 15: Displacement of the main beam

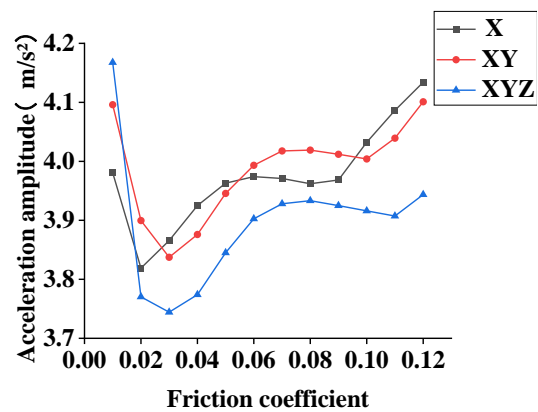


Fig. 16: Acceleration of the main beam

Figure 15 illustrates that as the friction coefficient of the friction pendulum escalates, the displacement of the main beam diminishes, with the rate of reduction progressively decreasing. This suggests that the enhancement of the friction

coefficient becomes increasingly ineffective in mitigating the displacement of the main beam. The displacements of the main beams in the XY and XYZ directions are essentially equivalent, with the maximum variance between different friction coefficients being 4.2%. Figure 16 illustrates that as the friction coefficient of the friction pendulum increases, the main beam acceleration trends for the three seismic wave input methods exhibit a similar pattern: initially decreasing and subsequently increasing. The minimum value occurs at a friction coefficient of approximately 0.02 to 0.03, indicating that the relationship between the friction coefficient and the main beam acceleration is not strictly linear.

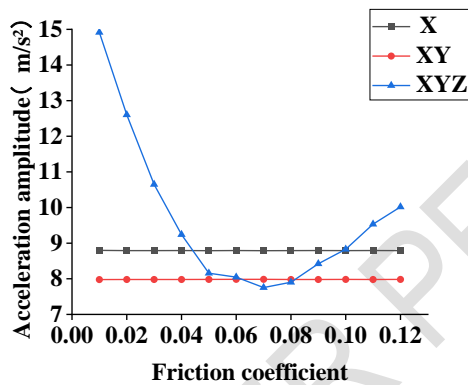


Fig. 17: Displacement of the pier top

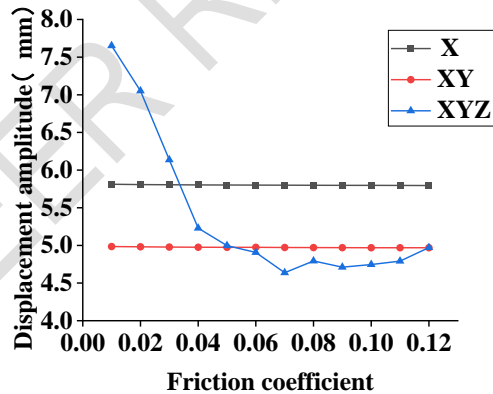


Fig. 18: Acceleration of the pier top

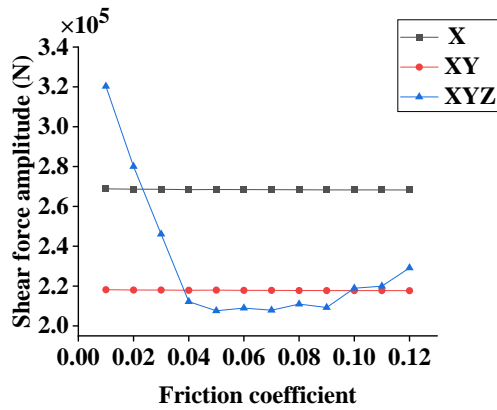


Fig. 19: Shear force at the pier bottom

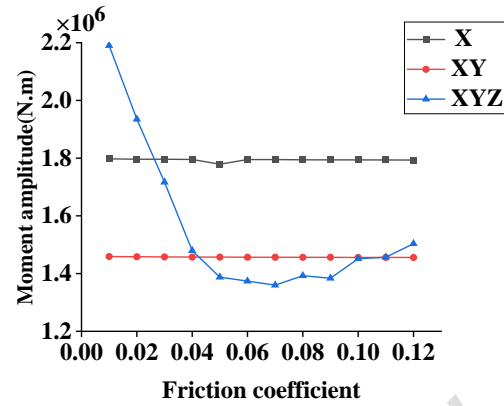


Fig. 20: Bending moment at the pier bottom

Figures 17 to 20 illustrate that as the friction coefficient of the friction pendulum increases, the displacement and acceleration at the top of the pier, as well as the shear force and bending moment at the bottom of the pier, exhibit similar trends across various seismic wave input modes. The X and XY directions remain largely unaffected by changes in the friction coefficient, while the XYZ direction initially decreases with increasing friction coefficient, followed by an increase, albeit at a rate lower than the initial decrease. Within a friction coefficient range of 0.05-0.08, the seismic response values at the top and bottom of the pier exhibit minimal variation. The minimal value is achieved at a friction coefficient of 0.07.

## 5 .Conclusions

This research primarily examines the influence of seismic wave characteristic period and friction pendulum friction coefficient on bridge parameters subjected to seismic waves of varying magnitudes, encompassing two primary components:

- (1) As the characteristic period of seismic waves increases, the displacement and acceleration values of the main girder exhibit a consistent trend throughout the three

seismic wave input modes, indicating that these modes have minimal impact on the main girder. The displacement and acceleration at the top of the pier, along with the shear force and bending moment at the base, exhibit a similar trend in the X and XY directions, while the XYZ direction demonstrates an increasing trend. Furthermore, the maximum rate of change in the XYZ direction significantly exceeds that of the X and XY directions, indicating that seismic waves in the Z direction exert a more pronounced influence on the displacement and acceleration at the top of the pier, as well as on the shear force and bending moment at the bottom.

(2) As the friction coefficient rises, the main beam displacement and acceleration exhibit similar patterns across various dimensions seismic wave inputs; specifically, the main beam displacement demonstrates a declining trend, whereas the main beam acceleration initially decreases before subsequently increasing. The displacement and acceleration at the top of the pier, along with the shear force and bending moment at the bottom, exhibit a consistent trend in the X and XY directions, with their magnitudes independent of the friction coefficient. Conversely, the XYZ direction initially decreases before increasing, with all values minimized at a friction coefficient of 0.07.

#### **Disclaimer (Artificial intelligence)**

Author(s) hereby declare that NO generative AI technologies such as Large Language Models (ChatGPT, COPILOT, etc.) and text-to-image generators have been used during the writing or editing of this manuscript.

#### **References**



- [1] Heydarpour, K., Tehrani, P., and Hariri-Ardebili, M. A. (2022). "Influence of Abutment Stiffness and Strength on the Seismic Response of Horizontally Curved RC Bridges in Comparison with Equivalent Straight Bridges at Different Seismic Intensity Levels." *Shock and Vibration*, 2022, 1-21.
- [2] Banerjee Basu, S., and Shinozuka, M. (2011). "Effect of Ground Motion Directionality on Fragility Characteristics of a Highway Bridge." *Advances in Civil Engineering*, 2011, 1-12.
- [3] Nielson, B. G., & DesRoches, R. (2007). Seismic performance assessment of simply supported and continuous multispan concrete girder highway bridges. *Journal of Bridge Engineering*, 12(5), 611-620.
- [4] Liang, X., and Mosalam, K. M. (2020). "Ground motion selection and modification evaluation for highway bridges subjected to Bi-directional horizontal excitation." *Soil Dynamics and Earthquake Engineering*, 130.
- [5] Caggiano, A., and Li, R. (2021). "Seismic vulnerability assessment of RC curved bridges piers subjected to bidirectional earthquake." *E3S Web of Conferences*, 293.
- [6] Cai, H., and Lu, H. (2019). "Dynamic response of long-span continuous curved box girder bridge under seismic excitation." *Journal of Vibroengineering*, 21(3), 696-709.
- [7] Thapa, S., Shrestha, Y., and Gautam, D. (2022). "Seismic fragility analysis of RC bridges in high seismic regions under horizontal and simultaneous horizontal and vertical excitations." *Structures*, 37, 284-294.

- [8] Shutong, C., Kassem, M. M., Jalilluddin, A. M., Mohamed Nazri, F., and Wenjun, A. (2023). "The effect of bridge girder-bearing separation on shear key pounding under vertical earthquake action – A state-of-the-art review." *Structures*, 55, 2445-2460.
- [9] Chen, S., Xia, H., An, W., Wen, Y., and Tornabene, F. (2021). "Theoretical Investigation on Multiple Separation of Bridge under Near-Fault Vertical Ground Motion." *Mathematical Problems in Engineering*, 2021, 1-15.
- [10] Zhang, Y., Ma, J., Chen, X., and Wang, Y. (2022). "Seismic response of the long-span steel truss arch bridge with the thrust under multidimensional excitation." *Railway Sciences*, 1(1), 40-55.
- [11] Li, Z., Wang, G., Fan, J., Wu, W., Jian, Y., Li, X., and Chung, W. (2022). "Seismic Response Analysis of Multidimensional and Multiangle Long-Span Top-Supported CFST Arch Bridge." *Advances in Civil Engineering*, 2022, 1-13.
- [12] Wang, S., Sun, Q., and Gao, H. (2020). "Dynamic Performance and Anti-earthquake Analysis of Cable-stayed Arch Bridge." *Journal of Civil, Construction and Environmental Engineering*, 5(2).
- [13] Gulerce, Z., Erduran, E., Kunnath, S. K., and Abrahamson, N. A. (2012). "Seismic demand models for probabilistic risk analysis of near fault vertical ground motion effects on ordinary highway bridges." *Earthquake Engineering & Structural Dynamics*, 41(2), 159-175.
- [14] Wilson, T., Chen, S., and Mahmoud, H. (2015). "Analytical case study on the seismic performance of a curved and skewed reinforced concrete bridge under

vertical ground motion." *Engineering Structures*, 100, 128-136.

- [15] Lei, Y., and Li, Q. (2016). "Experimental study on Y-shaped bridge under 3-dimensional earthquake ground motions." *KSCE Journal of Civil Engineering*, 21(6), 2329-2337.
- [16] Gu, Z.-y., Wang, S.-g., Liu, W.-q., Du, D.-s., and Xu, W.-z. (2017). "Experimental research and numerical simulation of a large-span isolated structure considering multi-dimensional input effects." *International Journal of Steel Structures*, 17(4), 1583-1595.
- [17] Zhang, H., Jiao, L., and Lin, J.-n. (2013). "Nonlinear analysis of pounding between decks of multi-span bridge subjected to multi-support and multi-dimensional earthquake excitation." *Journal of Central South University*, 20(9), 2546-2554.
- [18] Wang, Z., Padgett, J. E., and Dueñas-Osorio, L. (2020). "Influence of Vertical Ground Motions on the Seismic Fragility Modeling of a Bridge-Soil-Foundation System." *Earthquake Spectra*, 29(3), 937-962.
- [19] Ni, Y., Chen, J., Teng, H., and Jiang, H. (2015). "Influence of earthquake input angle on seismic response of curved girder bridge." *Journal of Traffic and Transportation Engineering (English Edition)*, 2(4), 233-241.
- [20] Ferreira, F., and Simões, L. (2022). "Optimum seismic design of curved cable-stayed bridges." *Structures*, 43, 131-148.
- [21] Gao, X. A., Zhou, X. Y., & Wang, L. (2004, August). Multi-component seismic analysis for irregular structures. In *13th World Conference on Earthquake*

*Engineering Vancouver, BC* (pp. 1-6).

- [22] Saxena, V., Deodatis, G., & Shinozuka, M. (2000, January). Effect of spatial variation of earthquake ground motion on the nonlinear dynamic response of highway bridges. In *Proc of 12th World Conf on Earthquake Engineering*.
- [23] Minavand, M., and Ghafory-Ashtiany, M. (2019). "Seismic Evaluation of Horizontally Curved Bridges Subjected to Near-Field Ground Motions." *Latin American Journal of Solids and Structures*, 16(2).
- [24] Computers and Structures, Inc. 1646 N. California Blvd., Suite 600, Walnut Creek, CA 94596, USA; 2020.
- [25] MOT (Ministry of Transport). Specifications for seismic design of highway bridges, Beijing, China; 2020.